Biochemical and Biophysical Research Communications 612 (2022) 181–187

Contents lists available at ScienceDirect

Biochemical and Biophysical Research Communications

journal homepage: www.elsevier.com/locate/ybbrc

Covalent binding of human two-domain CD4 to an HIV-1 subtype C SOSIP.664 trimer modulates its structural dynamics

Nancy L. Tumba [a], Previn Naicker [b], Stoyan Stoychev [b], Mark A. Killick [a], Gavin R. Owen [a, *], Maria A. Papathanasopoulos [a]

[a] HIV Pathogenesis Research Unit, Department of Molecular Medicine and Haematology, Faculty of Health Sciences, University of the Witwatersrand, 7 York Road, Parktown, 2193, Johannesburg, South Africa
[b] Council for Scientific and Industrial Research, Biosciences, Pretoria, 0001, South Africa

ARTICLE INFO

Article history:
Received 1 April 2022
Accepted 21 April 2022
Available online 26 April 2022

Keywords:
Hydrogen-deuterium exchange
HIV-1 subtype C SOSIP.664 trimer
Cluster of differentiation 4
HIV-1 vaccine immunogen
Protein dynamics

ABSTRACT

The human immunodeficiency virus type 1 (HIV-1) envelope glycoprotein (Env) mediates host cell infection by binding to the cellular receptor CD4. Recombinant Env bound to CD4 has been explored for its potential as an HIV vaccine immunogen as receptor binding exposes otherwise shielded, conserved functional sites. Previous preclinical studies showed an interchain disulphide linkage facilitated between Env and 2dCD4^{S60C} generates an immunogenic complex that elicits potent, broadly neutralizing antibodies (bNAbs) against clinically relevant HIV-1. This study investigated conformational dynamics of 2dCD4^{WT} and 2dCD4^{S60C} bound to an HIV−1C SOSIP.664 Env trimer using hydrogen-deuterium exchange mass spectrometry. The Env:2dCD4^{S60C} complex maintains key contact residues required for MHCII and Env/gp120 binding and the residues encompassing Ibalizumab's epitope. Important residues remaining anchored, with an increased flexibility in surrounding regions, evidenced by the higher exchange seen in flanking residues compared to Env:2dCD4^{WT}. While changes in Env:2dCD4^{S60C} dynamics in domain 1 were moderate, domain 2 exhibited greater variation. Lack of stability-inducing H-bonds in these allosteric sites suggest the improved immunogenicity of Env:2dCD4^{S60C} result from exposed CD4 residues providing diverse/novel antigenic targets for the development of potent, broadly neutralizing Ibalizumab-like antibodies.

1. Introduction

Human Immunodeficiency Virus type 1 (HIV-1) is composed *inter alia* of the envelope glycoproteins (Env) extracellular gp120 and transmembrane gp41 components non-covalently associated as heterodimeric trimers into the viral lipid bilayer [1]. HIV-1 infects host cells by initially binding of gp120 to the CD4 receptor on the surface of CD4^{+} T-cells. CD4 binding induces considerable conformational changes in gp120, enabling binding to CCR5 or CXCR4 [2]. From a therapeutic and vaccine development perspective, these co-receptor binding site epitopes as well as other CD4-induced (CD4i) sites are favourably exposed in the CD4-bound state.

Vaccine constructs based solely on Env monomers, trimers or SOSIP.664 trimers have poor immunogenicity in preclinical and human trials [3–9]. This is largely attributed to the extent of antibody somatic hypermutation required to generate potency and breadth over time, an invariably strong feature of HIV-1 bNAbs not yet replicable in a vaccine context. Thus, novel immunogen strategies and immunization protocols are being interrogated. While soluble CD4 (sCD4) in various forms has been investigated as candidate vaccines and therapeutics [10,11], a noteworthy vaccine strategy involves the use of Env:CD4 complexes. Covalently cross-linked complexes of Env to sCD4 did not generate autoimmunity but generated neutralizing antibodies against primary HIV-1 isolates following immunization of NHPs [12]. Similarly, we reported vaccine immunogens based on gp120 or gp140 conformations covalently complexed to a S60C mutant (2dCD4^{S60C}) eliciting bNAbs targeting the more neutralization-resistant (Tier-2 and -3) viruses

Abbreviations: 2dCD4, two domain CD4; CD4, cluster of differentiation 4; CD4bs, CD4 binding site; HDX-MS, hydrogen-deuterium exchange mass spectrometry; HIV-1, human immunodeficiency virus type 1; HPLC, High performance liquid chromatography; gp120, envelope glycoprotein 120 kDa; MHCII, major histocompatibility complex class II.

* Corresponding author.
E-mail address: Gavin.Owen@wits.ac.za (G.R. Owen).

https://doi.org/10.1016/j.bbrc.2022.04.101
0006-291X/

in New Zealand white rabbits [13]. Interestingly, the bNAb activity was largely directed towards Env:2dCD4^{S60C}, whereas the matched Env:2dCD4^{WT} showed a less efficient antibody response [13]. As determined by computational modelling, the substituted cysteine in 2dCD4^{S60C} enables a targeted disulphide exchange with the Cys126-Cys196 disulphide bridge on gp120, forming a Cys60-Cys126^{gp120} bond [14], which likely locks Env:2dCD4^{S60C} complexes in a conformation displaying conserved or novel epitopes. To understand the mechanisms underlying the improved antigenicity of the Env:2dCD4^{S60C}, we need to interrogate its conformational dynamics.

Thus, this study elucidated differences in conformational dynamics of SOSIP.664 trimers non-covalently bound to 2dCD4^{WT} or covalently bound to 2dCD4^{S60C} to provide conformational insights contributing to improved immunogenicity of Env:2dCD4^{S60C} in the context of 2dCD4, as determined by amide hydrogen-deuterium exchange coupled to mass spectrometry (HDX-MS).

2. Materials and methods

2.1. Hydrogen-deuterium exchange mass spectrometry (HDX-MS)

Differences between the non-covalently bound HIV−1C SOSIP.664gp140:2dCD4^{WT} complex (hereafter referred to as Env:2dCD4^{WT}) and covalently bound Env:2dCD4^{S60C} were compared by HDX-MS, using the automated LEAP PAL HDX system (Leap Technologies) coupled to an Agilent 1100 HPLC system and Sciex 6600 TripleTOF mass spectrometer. The amide hydrogen-deuterium exchange reaction was initiated by mixing 4 μl of Env:2dCD4^{WT} or Env:2dCD4^{S60C} with 16 μl 100% deuterated water at 4 °C. Three labelling time-points were used between 15 and 3600 s of exchange, after which 20 μl of the reaction mix was added to 30 μl of 1.7 M guanidium hydrochloride with 20 mM TCEP and 0.1% (v/v) formic acid to quench the reaction. Non-deuterated controls included substituting deuterated water with MilliQ water, and fully deuterated controls included proceeding with the exchange reaction overnight. Quenched samples were passed through a Poroszyme pepsin column (Life Technologies) (2.1 × 5 mm; flow rate, 100 μl/min) for proteolytic digestion, and the peptic fragments were desalted and separated on a Aeris peptide XBC18 column (2.1 × 5 mm) (linear gradient of 10–40% acetonitrile at a flow rate of 200 μl/min for 10 min). Eluted peptides were analysed on the AB Sciex 6600 TripleTOF mass spectrometer. For peptide identification the 6600 TripleTOF was operated in Data Dependant Acquisition (DDA) mode while for deuterium labelling only a precursor scan was collected. In DDA mode precursor scans were acquired from m/z 360–1500 using an accumulation time of 250 ms followed by 30 product scans, acquired from m/z 100–1800 at 100 ms each, for a total scan time of 3.3 s. Charge ions (1+ - 5+, that fall in the mass range 360–1500 m/z) were automatically fragmented in Q2 collision cells using nitrogen as the collision gas. Collision energies were chosen automatically as function of m/z and charge. Dynamic exclusion was set to 15 s. HDX-MS experiments were done in duplicate.

Data analysis and other methods can be found in supplementary methods.

3. Results

Partially deglycosylated HIV−1C SOSIP.664 gp140 was successfully expressed, purified and complexed to 2dCD4^{WT} or 2dCD4^{S60C} (Supplementary Fig. S1), and the conformational dynamics of the purified Env:2dCD4^{WT} or Env:2dCD4^{S60C} complexes were analysed by HDX-MS. Sequence coverage of 87% from 55 unique peptides were obtained for the 2dCD4 portion of the complexes (Supplementary Figs. S2 and S6). Conclusive analysis was not achieved for the Env portions of the complexes as the peptic fragments obtained for Env were insufficient for detailed interrogation.

3.1. Minimal changes in D1 of Env:2dCD4^{S60C} do not map to functionally important residues

The 2dCD4 portion of the complexes displayed differences in the rate of exchange between Env:2dCD4^{WT} and Env:2dCD4^{S60C} complexes in D1, particularly over one peptide (47–56) (Fig. 1). In this peptide, there was a 28% difference in deuterium incorporation along residues Gly41 to Leu44 and a 58% difference in Gly47 with the Env:2dCD4^{S60C} displaying rapid exchange from the first (15s) time-point compared to a more gradual deuteration in Env:2dCD4^{WT} (Supplementary Figs. S3 and S4). This implies that these residues are relatively buried in the non-covalent complex but patently solvent exposed in the covalent complex.

Some residues showed little to no difference between covalently and non-covalently bound complexes. This was the case for the mutated S60C residue having no deuteration for any of the time-points (Supplementary Fig. S3), while Lys35-a residue essential for MHCII binding-showed marginal deuterium uptake in both 2dCD4^{S60C} and 2dCD4^{WT} (0–16% and 11–29%, respectively) (Supplementary Figs. S3 and S4). Overall, changes in D1 indicate conformational differences resulting from a subtle loss of structural integrity in a few residues.

Full deuteration was observed in Env:2dCD4^{S60C} for the aromatic Phe43 residue (critical for Env binding) for all time-points assayed, while this residue displayed high (but not full) deuteration in Env:2dCD4^{WT} (68% - 15s, 71% - 5 min, and 72% - 60 min) (Supplementary Figs. S3 and S4). This lack of extensive differences in deuterium uptake between Env:2dCD4^{S60C} and Env:2dCD4^{WT} in D1 signals that the changes in dynamics are localised. Thus, the shift from protection to exposure in and around β-strand C″, triggered by the covalent bond formation between 2dCD4^{S60C} and Env is confined to the single peptide (47–56) notwithstanding a few allosteric effects.

3.2. Changes in conformational dynamics of residues at the 2dCD4 D1 and D2 interface induced by the Cys60-Cys126^{gp120} bond reveal how changes could be propagated across the domains

Within the interconnecting CD4 strand, where the G strand of D1 leads into the A strand of D2, three peptides (96–106; 103–111; and 105–113) show significant differences in deuteration (Fig. 1). These changes were mapped to Phe98, Thr101, Ser104, Asp105 and Gly111 (Fig. 2 and Supplementary Figs. S3 and S4). All these residues were fully deuterated for Env:2dCD4^{S60C} from the earliest timepoint and although all show 100% deuteration at the highest timepoint (60 min) for Env:2dCD4^{WT}, levels of deuteration varied widely at 15s mark (0% for Phe98 and Gly111; 61% for Thr101) (Supplementary Figs. S3 and S4). Other differences included Ser104 and Asp105, where there was no exchange for Ser104 except at 60 min (only 55%) in Env:2dCD4^{WT}, in contrast to full deuteration for all time-points in Env:2dCD4^{S60C} and comparatively less exchange for Asp105 (41–61%) in Env:2dCD4^{WT} (Supplementary Figs. S3 and S4). Differences in deuterium uptake on these three residues indicate this local environment experienced changes allowing for greater solvent accessibility in Env:2dCD4^{S60C}.

3.3. Covalent binding of Env:2dCD4^{S60C} increases the flexibility of CD4 D2

Several changes in deuteration levels was seen in D2, particularly in and between strands A and B, strand E, and in the G strand

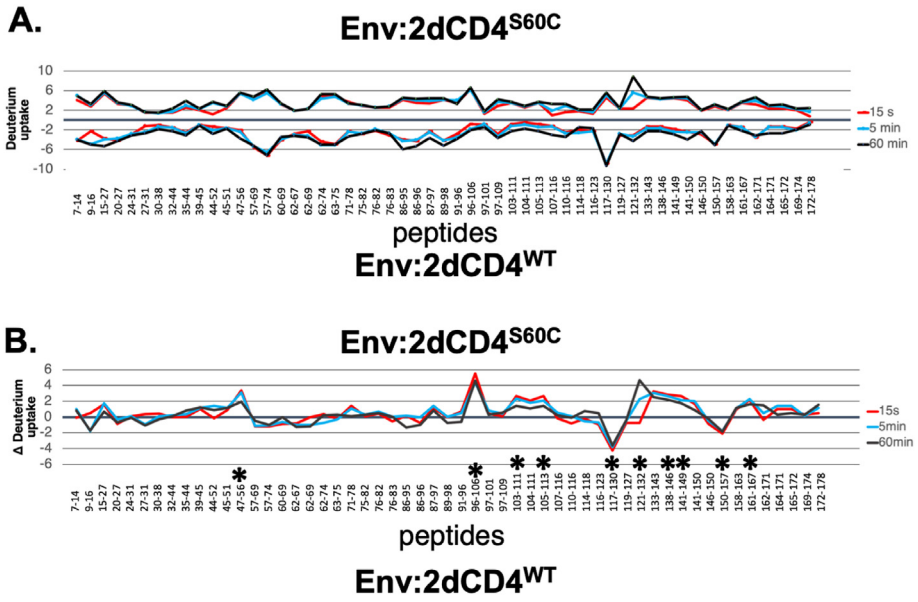

Fig. 1. Deuterium exchange profile of Env:2dCD4^{S60C} and Env:2dCD4^{WT} across all peptides. (A) Butterfly mirror and (B) difference plots comparing average deuterium incorporation for each peptide after 15s (red), 5 min (blue) and 60 min (black) deuteration. Lines above zero show uptake in Env:2dCD4^{S60C} while lines below zero show uptake for Env:2dCD4^{WT}. * denote peptides showing differences >2 Da. (For interpretation of the references to colour in this figure legend, the reader is referred to the Web version of this article.)

(Supplementary Figs. S3 and S4). Differences in the exchange rate of the D2 residues was extensive but concentrated in three regions: strands A and B with the loop between (region 1); strands C and E and a few adjoining residues (region 2); and strand G (region 3) (Figs. 1 and 3). Structurally, the amides in these residues do not appear to be involved in hydrogen bonding outside of the secondary structures where they reside, as such, electrostatic effects and solvent accessibility may be responsible for the protection seen in Env:2dCD4^{WT}. Noticeably, six peptides (117–130; 121–132; 138–146; 141–149; 150–157; and 161–167) displayed significant heterogeneity between Env:2dCD4^{S60C} and Env:2dCD4^{WT} (Fig. 1). Of these, 117–130 and 150–157 showed greater solvent exposure in Env:2dCD4^{WT} compared to Env:2dCD4^{S60C}.

The first region encompasses some of the residues discussed in the interdomain section above along with Leu116 whose solvent exposure occurred more rapidly in Env:2dCD4^{WT} than in Env:2dCD4^{S60C} (only at 15s), in contrast to the other changes seen in D2 (Supplementary Figs. S3 and S4). In addition, Thr111 was fully exposed (100% exchange) for the duration of the experiment in Env:2dCD4^{S60C} with full protection for this residue in the first two time-points for Env:2dCD4^{WT} (100% deuteration at 60 min). Similarly, Leu114 also supported full protection in Env:2dCD4^{WT} but was solvent exposed at 60 min for Env:2dCD4^{S60C} (Supplementary Figs. S3 and S4). This indicates that Env:2dCD4^{WT} sustained some level of protection in this region whereas Env:2dCD4^{S60C} exposed these residues except for Leu116 which remained anchored.

The second region includes residues surrounding Cys130 (a residue involved in a −RHstaple disulphide bond with Cys159 (Fig. 4) whose redox state dictates the functionality of CD4 [14,15,16]). No differences were seen for Cys130. Levels of deuteration in Arg131 and Ser132 was higher for the first two time-points in Env:2dCD4^{WT} compared to Env:2dCD4^{S60C} (Fig. 4), indicating structural protection in the covalent complex. Peptic fragments covering Cys159 were insufficient to conclusively determine its level of deuteration. Ser145, Ser147, and Glu150 were fully deuterated from 15s in Env:2dCD4^{S60C} while all three residues gained deuterons relatively slowly over time in Env:2dCD4^{WT} reaching 78% (Ser145), 67% (Ser147), and 100% (Glu150) deuterium uptake (Supplementary Figs. S3 and S4). This indicates Env:2dCD4^{WT} is protected in this D2 region whereas Env:2dCD4^{S60C} exposed these residues while maintaining the adjoining F strand static/shielded (Fig. 4).

The third region contains D2 β-strand G where several peptides show increased deuterium uptake in Env:2dCD4^{S60C} relative to Env:2dCD4^{WT} (Figs. 1, 3 and 4). Predominantly, Lys167 and Ile172 were fully deuterated in Env:2dCD4^{S60C} with gradual increases in deuteration in Env:2dCD4^{WT}. Leu177 displayed gradual deuteration for both Env:2dCD4^{S60C} and Env:2dCD4^{WT} with the covalent complex reaching full deuteration compared to the non-covalent complex only reaching 14% deuteration at the highest timepoint. Overall, the higher deuterium incorporation in the G strand on Env:2dCD4^{S60C} indicates higher solvent accessibility or enhanced flexibility compared to Env:2dCD4^{WT}. The lack of potential H-bonding interactions in this region indicates a general trend towards the G strand being less rigid or having a diminished burial depth in the Env:2dCD4^{S60C}.

From an immunological standpoint, Ibalizumab binds to CD4 D2 and of the four amino acids comprising the epitope (Glu77, Pro121, Pro122, Gln163), only Gln163 showed differential exchange-gradual deuteration in Env:2dCD4^{WT} (39%, 42%, 75%) compared to rapid exchange in Env:2dCD4^{S60C} (Figs. 1 and 2). This indicates that Gln163 is slightly more exposed in Env:2dCD4^{S60C}. The lack of difference in deuteration for the Ibalizumab epitope (aside from the Gln163 residue) between the two 2dCD4 variants indicates that the introduction of the covalent bond with 2dCD4^{S60C} did not structurally impede the presentation of the antigenic residues comprising the Ibalizumab epitope.

4. Discussion

HIV-1 vaccine design studies encourage the presentation of immunodominant epitopes that are conserved amongst clinically relevant circulating HIV-1 subtypes worldwide. Our previous studies revealed that covalently complexed Env:2dCD4^{S60C} resulted

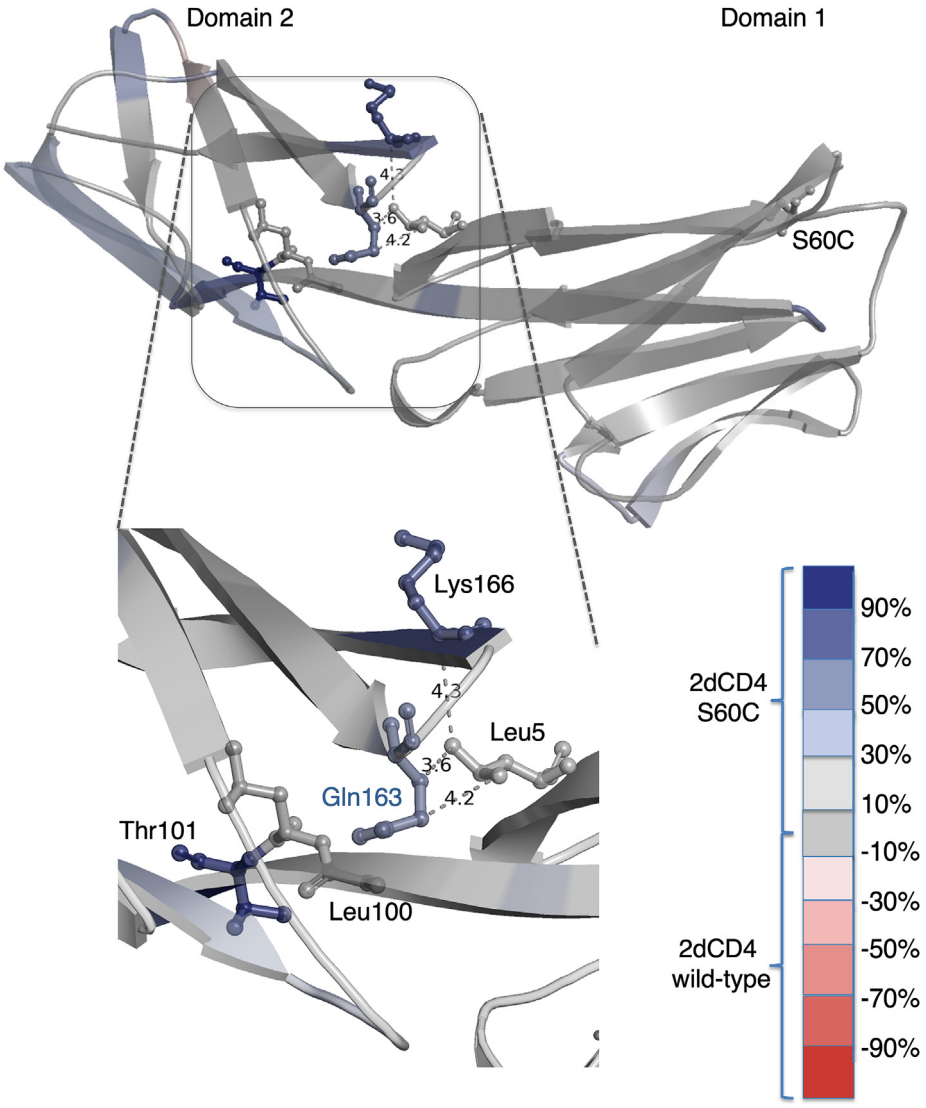

Fig. 2. Deuterium uptake differences between Env:2dCD4^{WT} and Env:2dCD4^{S60C} at the CD4 D1 and D2 interface. Relative deuteration (at 5 min) mapped onto the 2dCD4 crystal structure (PDB: 1CDJ**). Some residues are shown as ball-and-stick and labelled with amino acid and residue number. Distances between Leu5 in D1 and the closest D2 residues are shown. A colour gradient was used where red and blue represent higher relative deuteration in Env:2dCD4^{WT} and Env:2dCD4^{S60C}, respectively**. (For interpretation of the references to colour in this figure legend, the reader is referred to the Web version of this article.)

in highly desirable bNAb activity [13]. Whether the targeted epitopes are novel or presented differently in Env:2dCD4^{S60C} versus Env:2dCD4^{WT} remains to be determined and may involve an increase in the stability of the complex, a change in conformational landscape, or epitope enhancement/diversification through an undetermined mechanism.

This study compared the conformational dynamics of Env:2dCD4^{S60C} and Env:2dCD4^{WT}. HIV−1C gp140 Env complexed to 2dCD4^{S60C} shows improved immunogenicity over the 2dCD4^{WT} complex in rabbits [13]. We hypothesised that the disulphide linkage in Env:2dCD4^{S60C} impacted structure-function by changing specific states of the Env:2dCD4^{S60C} complex thereby exposing unique epitopes by inducing different conformational dynamics to the Env:2dCD4^{WT}.

2dCD4 has disulphide bonds in both D1 and D2. Reducing the metastable, allosteric D2 disulphide is necessary for Env binding, evidenced by the fact that it is impossible for Env to bind a CD4 molecule with an oxidized D2 disulphide [14,16]. Also, the D1 disulphide is a structural bond whose reduction has deleterious effects on CD4 structure [17]. The low concentration (1 mM) of β-mercaptoethanol used to facilitate exchange and formation of the Cys60-Cys126^{gp120} bond in Env:2dCD4^{S60C} was unlikely to alter the gp120 bound redox state of either D1 or D2 disulphides. If it had, a reduced D1 disulphide would result in a conformationally disrupted protein unable to interact with Env, while a reduced D2 disulphide was congruent with the binding of CD4 to gp120. Thus, addition of 1 mM β-mercaptoethanol to Env:2dCD4^{S60C} has not incurred changes to the complex outside of facilitating the Cys60-Cys126^{gp120} disulphide link.

Published studies examining dynamics and immunogenicity of gp120:CD4 complexes have focused on gp120 [18–20]. By contrast, this study evaluated the structural dynamics of 2dCD4 in the context of covalent and non-covalent binding to an HIV−1C SOSIP.664 gp140. Analysis did not extend to the Env portion due to low peptide coverage for those regions. Another acknowledged limitation in the experimental setup was the failure to include unliganded 2dCD4$^{WT/S60C}$ as controls. Substantial information is available on the conformational dynamics of unliganded 2dCD4,

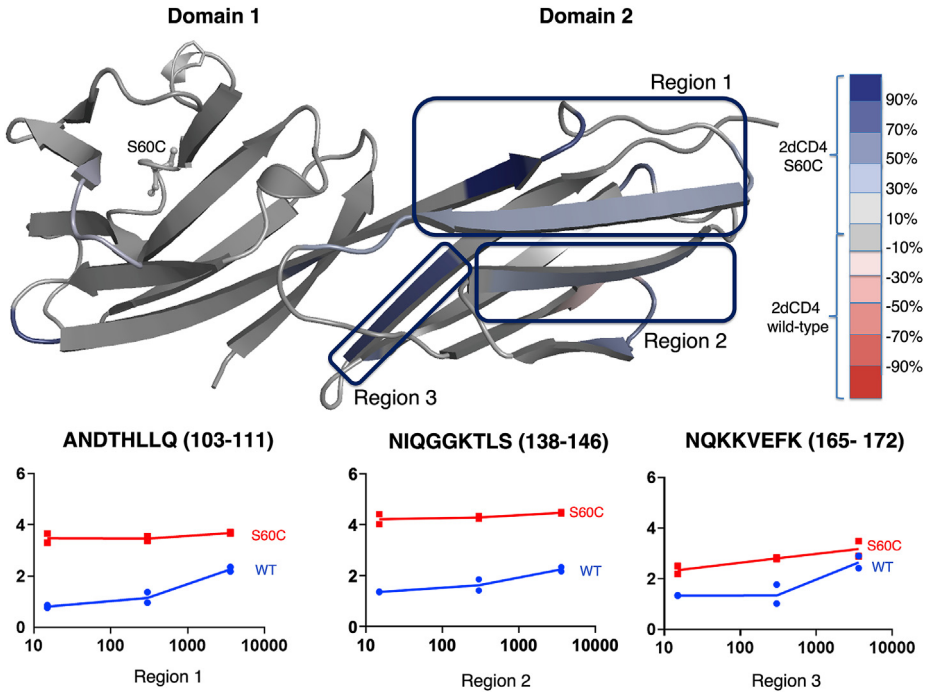

Fig. 3. Deuterium uptake differences between Env:2dCD4^{S60C} and Env:2dCD4^{WT} after 5 min labelling mapped onto the 3D structure of 2dCD4. Regions with the highest amount of variations in deuterium incorporation are boxed and labelled. Selected plots showing relative deuterium content for representative peptic fragments are shown. The 2dCD4^{WT} curves are shown in blue and 2dCD4^{S60C} curves in red. Each replicate bullet point is represented. Position of S60C is shown in ball and stick. For the ribbon structure, the colour scale represents change in percentage deuteration from Env:2dCD4^{S60C} to Env:2dCD4^{WT} with higher relative deuteration indicated in red in Env:2dCD4^{S60C} and blue in Env:2dCD4^{WT}. (For interpretation of the references to colour in this figure legend, the reader is referred to the Web version of this article.)

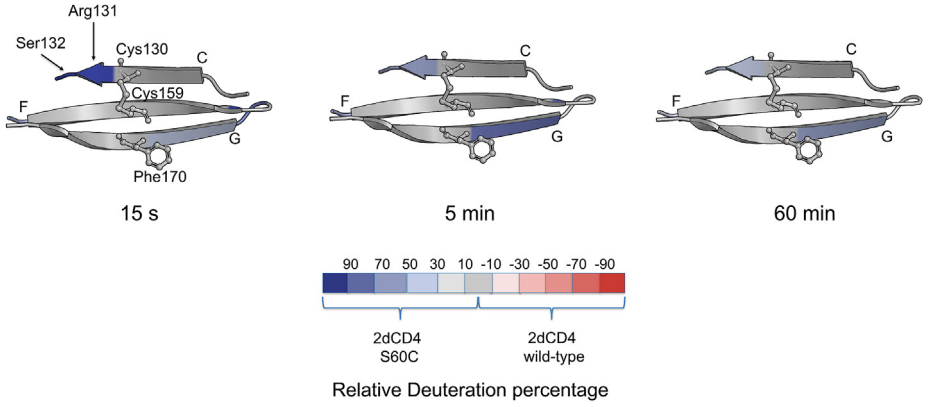

Fig. 4. Deuterium incorporation differences in the C, F, and G strands of D2 for Env:2dCD4^{S60C} and Env:2dCD4^{WT}. β-strands (labelled C, F and G) are depicted with cysteine residues making up the allosteric bond and the G-strand phenylalanine represented in ball-and-stick format. Also labelled are C-strand residues Arg131 and Ser132. Colours show difference in deuteration according to the scale, with higher relative deuteration in red in Env:2dCD4^{WT} and blue in Env:2dCD4^{S60C}. (For interpretation of the references to colour in this figure legend, the reader is referred to the Web version of this article.)

including the effects of D1 and D2 disulphide ablation on the structural conformation of 2dCD4 [14,17,21]. As such, this study focused on the differences observed between Env:2dCD4^{WT} and Env:2dCD4^{S60C} for the CD4 component, in the context of an intact D1 disulphide and a reduced D2 disulphide.

Most functionally relevant residues displayed little to no change between Env:2dCD4^{S60C} and Env:2dCD4^{WT}. This was the case for Lys35 and Phe43 (a residue involved in binding gp120) had slight differences in deuteration, although deuteration was high in this residue for both Env:2dCD4^{S60C} or Env:2dCD4^{WT}. Thus, the formation of the directed disulphide bond, likely does not affect the integrity of interaction between gp120 and 2dCD4.

Most differences in dynamics between Env:2dCD4^{S60C} and Env:2dCD4^{WT} were seen in D2. D1 had minor differences observed in a single peptide whose comparatively small fluctuations may be indicative of changes prompted by the introduction of the cysteine at position 60 and the resultant covalent linkage. These oscillations were propagated through the network of interactions across the length of the protein with changes in interdomain, bridging residues (Fig. 2). This assumedly resulted in the evident alterations seen in D2. Changes in D2 were evidenced by its acquired solvent exposure and deduced enhanced flexibility (Supplementary Fig. S5).

The redox biology of CD4 in the context of Env binding is well characterised [14,15,16]. D2 of CD4 has an unusual Cys130-Cys159 allosteric disulphide bond that connects adjacent strands [16,22],

and is reduced natively by thioredoxin secreted on $CD4^+$ T-cells [15]. Reduction of the Cys130-Cys159 disulphide causes the β-strands surrounding it to slightly collapse inwardly leading to a spatially diminished, stable molecule with decreased dynamics [21]. Both protein complexes were size-exclusion purified as 2dCD4-bound SOSIP.664 trimer complexes and as such, the D2 Cys130-Cys159 disulphide would have been reduced in both as required for gp120 binding. The lack of dynamic changes for Cys130 in Env:2dCD4^{S60C}, combined with the changes for the two residues directly following, is interesting as it indicates that disruption by the Cys60-Cys126^{gp120} covalent bond had no detectable effect on Cys130 yet caused a shift in the network of residues directly following Cys130. Thus the S60C-induced covalent bond may act as a stabilizing disulphide, allowing the shielding of some residues while exposing surrounding ones for a more dynamic presentation of additional conformations. Thus Env:2dCD4^{S60C} presents the 2dCD4 component in its reduced isoform (similar to Env:2dCD4^{WT}) but the covalent complex displays the increased dynamics of an oxidized D2 disulphide, generating an attractive vaccine immunogen target. Flexibility of D2 is well described in the context of gp120 binding and the high dynamics of D2 observed in Env:2dCD4^{S60C} was fitting for this flexible domain. These changes may be directly causative or may contribute to the difference in immunogenicity of Env:2dCD4^{S60C} compared to Env:2dCD4^{WT}.

Results imply that covalently linking 2dCD4^{S60C} with Env resulted in effective stabilization of conformation(s) that, albeit more transiently present in Env:2dCD4^{WT} may cause prolonged exposure of epitopes in Env:2dCD4^{S60C}. The potent bNAb responses from rabbits immunized with Env:2dCD4^{S60C} were largely attributed to the 2dCD4-directed component [13], in agreement with the abovementioned hypothesis. Thus, covalently linking the two molecules further increases the dynamics and conformational flexibility of D2 in 2dCD4, conducive with the generation of bNAbs that are potentially directed against novel 2dCD4^{S60C} epitopes.

Ibalizumab is a humanized Mab, a CD4-directed post-attachment HIV-1 inhibitor that is FDA approved for use in treatment-experienced adults with multidrug resistant HIV-1 infection. The Ibalizumab epitope is formed by amino acid residues in D2 of CD4: Leu96, Pro121, Pro122 and Gln163 as well as Glu77 and Ser79 in D1, opposite the site where gp120 and the MHC class II molecule bind in D1. We hypothesize the potent, bNAb activity elicited by our Env:2dCD4^{S60C} immunogen is Ibalizumab-like. The HDX-MS data supports this hypothesis by confirming the stable exposure of relevant Ibalizumab epitopes yet a disruption of networks surrounding this epitope in Env:2dCD4^{S60C}. This result was slightly unexpected as residues involved in intermolecular interactions with binding partners tend to be solvent exposed, enabling hydrogen binding and proton transfer. However, maintaining the integrity of the Ibalizumab epitope and the interface for binding partners such as HIV-1 gp120 and MHCII suggests the immunogen would not likely cause immunosuppression.

We set out to determine differences in conformational dynamics of Env:2dCD4^{S60C} and Env:2dCD4^{WT}. In this scenario, the S60C-assisted covalent bond triggers a network of changes that slightly disrupts D1 stability but increases the dynamics of D2 of 2dCD4. These results highlight the conformational dynamics differences between Env:2dCD4^{S60C} and Env:2dCD4^{WT} and reveal the structural mechanisms behind these novel CD4-bound immunogens which consistently induced potent, HIV-specific bNAbs in preclinical testing. Our findings provide important insights into the highly immunogenic residues of our vaccine immunogens.

Funding

Research was supported by grants from the Department of Molecular Medicine and Haematology, the Poliomyelitis Research Foundation, and the South African National Research Foundation through a Thuthuka grant.

Declaration of competing interest

The authors declare that they have no known competing financial interests or personal relationships that could have appeared to influence the work reported in this paper.

Appendix A. Supplementary data

Supplementary data to this article can be found online at https://doi.org/10.1016/j.bbrc.2022.04.101.

References

[1] R.J. Center, R.D. Leapman, J. Lebowitz, L.O. Arthur, P.L. Earl, B. Moss, Oligomeric structure of the human immunodeficiency virus type 1 envelope protein on the virion surface, J. Virol. 76 (2002) 7863–7867.
[2] L.T. Da, J.M. Quan, Y.D. Wu, Understanding of the bridging sheet formation of HIV-1 glycoprotein gp120, J. Phys. Chem. B 113 (2009) 14536–14543, https://doi.org/10.1021/jp9081239.
[3] B.K. Chakrabarti, Y. Feng, S.K. Sharma, K. McKee, G.B. Karlsson Hedestam, C.C. Labranche, D.C. Montefiori, J.R. Mascola, R.T. Wyatt, Robust neutralizing antibodies elicited by HIV-1 JRFL envelope glycoprotein trimers in nonhuman primates, J. Virol. 87 (2013) 13239–13251, https://doi.org/10.1128/JVI.01247-13.
[4] R.W. Sanders, M.J. van Gils, R. Derking, D. Sok, T.J. Ketas, J.A. Burger, G. Ozorowski, A. Cupo, C. Simonich, L. Goo, H. Arendt, H.J. Kim, J.H. Lee, P. Pugach, M. Williams, G. Debnath, B. Moldt, M.J. van Breemen, G. Isik, M. Medina-Ramírez, J.W. Back, W.C. Koff, J.P. Julien, E.G. Rakasz, M.S. Seaman, M. Guttman, K.K. Lee, P.J. Klasse, C. LaBranche, W.R. Schief, I.A. Wilson, J. Overbaugh, D.R. Burton, A.B. Ward, D.C. Montefiori, H. Dean, J.P. Moore, HIV-1 VACCINES. HIV-1 neutralizing antibodies induced by native-like envelope trimers, Science 349 (2015), aac4223, https://doi.org/10.1126/science.aac4223.
[5] P. Martinez-Murillo, K. Tran, J. Guenaga, G. Lindgren, M. Àdori, Y. Feng, G.E. Phad, N. Vázquez Bernat, S. Bale, J. Ingale, V. Dubrovskaya, S. O'Dell, L. Pramanik, M. Spångberg, M. Corcoran, K. Loré, J.R. Mascola, R.T. Wyatt, G.B. Karlsson Hedestam, Particulate array of well-ordered HIV clade C Env trimers elicits neutralizing antibodies that display a unique V2 cap approach, Immunity 46 (2017) 804–817, https://doi.org/10.1016/j.immuni.2017.04.021, e807.
[6] L. He, S. Kumar, J.D. Allen, D. Huang, X. Lin, C.J. Mann, K.L. Saye-Francisco, J. Copps, A. Sarkar, G.S. Blizard, G. Ozorowski, D. Sok, M. Crispin, A.B. Ward, D. Nemazee, D.R. Burton, I.A. Wilson, J. Zhu, HIV-1 vaccine design through minimizing envelope metastability, Sci. Adv. 4 (2018), https://doi.org/10.1126/sciadv.aau6769 eaau6769.
[7] N.M. Flynn, D.N. Forthal, C.D. Harro, F.N. Judson, K.H. Mayer, M.F. Para, rgp120 HIV Vaccine Study Group, Placebo-controlled phase 3 trial of a recombinant glycoprotein 120 vaccine to prevent HIV-1 infection, J. Infect. Dis. 191 (2005) 654–665, https://doi.org/10.1086/428404.
[8] S. Rerks-Ngarm, P. Pitisuttithum, S. Nitayaphan, J. Kaewkungwal, J. Chiu, R. Paris, N. Premsri, C. Namwat, M. de Souza, E. Adams, M. Benenson, S. Gurunathan, J. Tartaglia, J.G. McNeil, D.P. Francis, D. Stablein, D.L. Birx, S. Chunsuttiwat, C. Khamboonruang, P. Thongcharoen, M.L. Robb, N.L. Michael, P. Kunasol, J.H. Kim, M.-T. Investigators, Vaccination with ALVAC and AIDSVAX to prevent HIV-1 infection in Thailand, N. Engl. J. Med. 361 (2009) 2209–2220, https://doi.org/10.1056/NEJMoa0908492.
[9] J. Abbasi, Large HIV vaccine trial launches in South Africa, JAMA 317 (2017) 350, https://doi.org/10.1001/jama.2016.20743.
[10] W. Chen, Y. Feng, R. Gong, Z. Zhu, Y. Wang, Q. Zhao, D.S. Dimitrov, Engineered single human CD4 domains as potent HIV-1 inhibitors and components of vaccine immunogens, J. Virol. 85 (2011) 9395–9405, https://doi.org/10.1128/JVI.05119-11.
[11] W. Chen, Y. Feng, P. Prabakaran, T. Ying, Y. Wang, J. Sun, C.D. Macedo, Z. Zhu, Y. He, V.R. Polonis, D.S. Dimitrov, Exceptionally potent and broadly cross-reactive, bispecific multivalent HIV-1 inhibitors based on single human CD4 and antibody domains, J. Virol. 88 (2014) 1125–1139, https://doi.org/10.1128/JVI.02566-13.
[12] T. Fouts, K. Godfrey, K. Bobb, D. Montefiori, C.V. Hanson, V.S. Kalyanaraman, A. DeVico, R. Pal, Crosslinked HIV-1 envelope-CD4 receptor complexes elicit broadly cross-reactive neutralizing antibodies in rhesus macaques, Proc. Natl. Acad. Sci. U. S. A. 99 (2002) 11842–11847, https://doi.org/10.1073/pnas.182412199.
[13] M.A. Killick, M.L. Grant, N.M. Cerutti, A. Capovilla, M.A. Papathanasopoulos, Env-2dCD4 S60C complexes act as super immunogens and elicit potent, broadly neutralizing antibodies against clinically relevant human immunodeficiency virus type 1 (HIV-1), Vaccine 33 (2015) 6298–6306, https://doi.org/

10.1016/j.vaccine.2015.09.056.
[14] N. Cerutti, M. Killick, V. Jugnarain, M. Papathanasopoulos, A. Capovilla, Disulfide reduction in CD4 domain 1 or 2 is essential for interaction with HIV glycoprotein 120 (gp120), which impairs thioredoxin-driven CD4 dimerization, J. Biol. Chem. 289 (2014) 10455–10465, https://doi.org/10.1074/jbc.M113.539353.
[15] L.J. Matthias, P.T. Yam, X.M. Jiang, N. Vandegraaff, P. Li, P. Poumbourios, N. Donoghue, P.J. Hogg, Disulfide exchange in domain 2 of CD4 is required for entry of HIV-1, Nat. Immunol. 3 (2002) 727–732, https://doi.org/10.1038/ni815.
[16] L.J. Matthias, I. Azimi, C.A. Tabrett, P.J. Hogg, Reduced monomeric CD4 is the preferred receptor for HIV, J. Biol. Chem. 285 (2010) 40793–40799, https://doi.org/10.1074/jbc.M110.190579.
[17] G.R. Owen, J.A. Channell, V.T. Forsyth, M. Haertlein, E.P. Mitchell, A. Capovilla, M. Papathanasopoulos, N.M. Cerutti, Human CD4 metastability is a function of the allosteric disulfide bond in domain 2, Biochemistry 55 (2016) 2227–2237, https://doi.org/10.1021/acs.biochem.6b00154.
[18] T.M. Davenport, M. Guttman, W. Guo, B. Cleveland, M. Kahn, S.L. Hu, K.K. Lee, Isolate-specific differences in the conformational dynamics and antigenicity of HIV-1 gp120, J. Virol. 87 (2013) 10855–10873, https://doi.org/10.1128/JVI.01535-13.
[19] M. Guttman, N.K. Garcia, A. Cupo, T. Matsui, J.P. Julien, R.W. Sanders, I.A. Wilson, J.P. Moore, K.K. Lee, CD4-induced activation in a soluble HIV-1 Env trimer, Structure 22 (2014) 974–984, https://doi.org/10.1016/j.str.2014.05.001.
[20] Y. Li, L. Deng, L.Q. Yang, P. Sang, S.Q. Liu, Effects of CD4 binding on conformational dynamics, molecular motions, and thermodynamics of HIV-1 gp120, Int. J. Mol. Sci. 20 (2019), https://doi.org/10.3390/ijms20020260.
[21] G.R. Owen, D. Le, S. Stoychev, N.M. Cerutti, M. Papathanasopoulos, Redox exchange of the disulfides of human two-domain CD4 regulates the conformational dynamics of each domain, providing insight into its mechanisms of control, Biochem. Biophys. Res. Commun. 497 (2018) 811–817, https://doi.org/10.1016/j.bbrc.2018.02.161.
[22] B. Schmidt, P.J. Hogg, Search for allosteric disulfide bonds in NMR structures, BMC Struct. Biol. 7 (2007) 49, https://doi.org/10.1186/1472-6807-7-49.